High Enrichment of ^{6}Li in Molten Nitrates by the Klemm Method

Isao Okada[a,b], Masao Nomura[a], and Teruo Haibara[a,c]

[a] Research Laboratory for Nuclear Reactors, Tokyo Institute of Technology, O-okayama, 2-12-1, Meguro-ku, Tokyo 152-8550, Japan

[b] Present address: Faculty of Science and Technology, Sophia University, 7-1 Kioi-cho, Chiyoda-ku, Tokyo 102-8554, Japan (Professor Emeritus of Tokyo Institute of Technology)

[c] Present address: Nippon Micrometal Corporation, Sayamagahara 158-1, Iruma-shi, Saitama 358-0032, Japan

Reprint requests to I. O.; Fax: +81-3-5357-8205, E-mail: i-okada@dol.hi-ho.ne.jp

Z. Naturforsch. **68a,** 21 – 38 (2013) / DOI: 10.5560/ZNA.2012-0104
Received August 26, 2012 / published online February 15, 2013

This paper is dedicated to Professor Alfred Klemm on the occasion of his 100th birthday

The Klemm method of isotopic enrichment (countercurrent electromigration of molten salts) and many of its implications are reviewed and discussed. On the basis of this principle, a small amount of ^{6}Li was enriched in some experiments from its original abundance, 7.6%, to 94.9% at about 300 °C. The variation of the conditions led to a modified setup where, by disposing a small amount of $NaNO_3$ between the catholyte (NH_4NO_3) and the zone of $LiNO_3$, the frontal part, where ^{6}Li is to be enriched, could be kept stable under high current density for more than one month without any problem of corrosion. The reasons and implications of this new step are discussed, underlining the up-to-dateness of Klemm's experiment.

Key words: Enrichment of ^{6}Li; Molten $LiNO_3$; The Klemm Method; The Chemla Effect; The Lundén Anomaly.

1. Introduction

Some 70 years ago, Klemm devised a countercurrent electomigration method in molten salts for enriching isotopes, particularly of alkali and alkaline earth elements [1, 2], which has been later named 'la méthode de Klemm' [3], Klemm's method [4] or the Klemm method [5]. This Klemm method may be regarded as a kind of the Hittorf method, as seen from a comparison of the principles of the Klemm (or column) method with the Hittorf (or disk) method [6] in Figure 1. However, the concentration change after electromigration particularly toward the anode is much larger in the Klemm method. One of the great advantages of this method in comparison with the one in aqueous solutions [7] is that countercurrent flow of cations occurs spontaneously owing to the gravity and the capillary action of the diaphragm. Therefore, in a binary mixture with a common anion, the less mobile cation is readily enriched at the anode side. Moreover, when the Chemla effect, which will be discussed below, occurs, the concentration (the mole fraction) of the cations tends toward the one corresponding to the Chemla crossing point, whereas the heavier isotopes continue to be enriched toward the anode.

Traditional applications of the Klemm method are shown in Figure 2. For the measurement of the isotope effect of two (cationic) isotopes 1 and 2 in pure melts, (1) can be applied [1]:

$$\varepsilon \equiv \frac{u_1 - u_2}{\langle u \rangle} = \frac{u_1 - u_2}{x_1 u_1 + x_2 u_2} = -\left(\frac{N_1}{N_1^0} - \frac{N_2}{N_2^0}\right)\frac{FN}{Q}, \quad (1)$$

where ε is the relative internal mobility difference of isotopes of 1 and 2, that is, the elementary separation factor; u_i is the internal mobility of isotope i, and x_i its mole fraction; N_i and N_i^0 are the quantities of i, respectively, after and before electromigration, contained in the vicinity of the anode, where the heavier isotope 2 is enriched against the lighter one 1; N is the total quantity of the anions contained there, Q the transported charge, and F the Faraday constant. The negative sign at the beginning of the rightmost term in (1) comes from the fact that the heavier isotope is enriched on the anode side. An advantage of the Klemm method

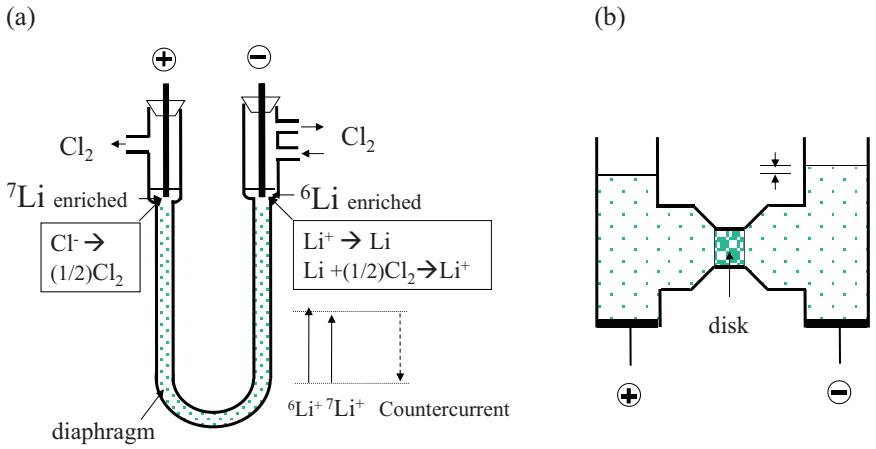

Fig. 1 (colour online). Schematic representation of the Klemm method (a) as compared with the Hittorf method (b). The reference frame of the velocities is the diaphragm, when the electric current is balanced by the countercurrent flow.

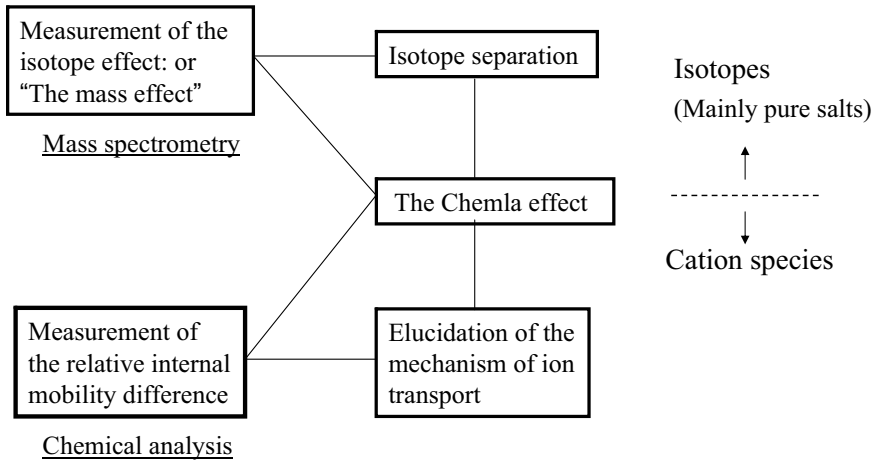

Fig. 2. Various experimental problem approaches related to the Klemm effect and their interrelations.

is suggested also by (1); the relative change from the initial values (i.e. the ratios of N_1/N_1^0 and N_2/N_2^0) is important, but knowledge of the absolute values of N_i or N_i^0 ($i = 1, 2$) is not necessarily required.

The isotope effect in this method has been defined by Klemm in the form of the 'mass effect' [8]: $-\mu = (\Delta b/b)/(\Delta m/m)$, where b ('Beweglichkeit') is the internal mobility, and m the mass; the negative sign comes from the fact that the lighter isotope is always more mobile than the heavier one. It was recommended later by the International Union of Pure and Applied Chemistry (IUPAC) [9] that the mobility should be expressed by u or μ; u is employed here instead of b, as given in (1), and μ is used for the mass effect in the present paper, as has been proposed by Klemm.

The mass effect is a convenient quantity for comparing the isotope effects among various cations; it has been measured for alkali and alkaline earth elements in many molten halides, nitrates, and so on, and even for some anions. The mass effect of various ions has been summarized by Klemm, for example, in [10 – 12].

Equation (1) can be applied even for trace amounts of radioisotopes; for example, even though sodium is mono-nuclidic, the isotope effect in the mobilities of Na^+ in $NaNO_3$ can be readily measured using the two radioisotopes ^{22}Na ($h_{1/2} = 2.60$ y) and ^{24}Na ($h_{1/2} = 14.66$ h) [13]. Whereas cesium (^{133}Cs) is mono-nuclidic like sodium, the mass effect for these ions has been determined in pure $CsNO_3$ by use of two radioisotopes, ^{132}Cs ($h_{1/2} = 6.475$ d) and ^{137}Cs ($h_{1/2} = 30.0$ y). The mass effects measured with

radioisotopes do not give anomalous values as compared with the ones of other alkali ions – lithium, potassium, and rubidium – measured with the stable isotopes [14].

In $Dy_{1/3}Cl$, the mass effect of the dysprosium isotopes has been measured at 700 – 800 °C to be $-\mu = 0.032 \pm 0.002$ from the main five isotopes out of seven (^{156}Dy: 0.06%, ^{158}Dy: 0.10%, ^{160}Dy: 2.34%, ^{161}Dy: 18.91%, ^{162}Dy: 25.51%, ^{163}Dy: 24.90%, and ^{164}Dy: 28.18%) [15]; this value is comparable to the ones of Rb^+ in $RbNO_3$ (0.033 at 350 °C [16]) and of Sr^{2+} in $Sr_{1/2}Cl$ (0.035 at 1000 °C [17]). From the relatively large positive value of $-\mu$, the main charge transporting species is inferred to be a cationic Dy^{3+} ion and not an anionic complex ion like e.g. $[DyCl_4]^-$. Thus, from measurement of the mass effect, one may determine whether the charge transporting species is a cation or a complex anion.

Incidentally, the external mobility has also been defined as the mobility of ions with respect to migration media such as a silicate disk. The mobility ratios of cations and anions correspond to the *external* transport numbers of the cations and the anions, respectively. Therefore, the *internal* cation mobility is the sum of the external mobilities of cation and anion. The external transport numbers are found to be dependent on the nature of the frit [18], and not to be intrinsic properties of the molten salt of interest. The external transport numbers cannot be measured by the Klemm method but by a modified Hittorf method [19]. In the present paper, the mobility refers to the internal mobility, unless noted otherwise.

Essentially the same equation as (1) can be applied for the relative difference in the internal mobilities of two cations in additive binary mixtures [1, 20], and also for each cation pair in additive ternary mixtures such as (Li, Na, K)NO_3 [21], (Li, K, Cs)NO_3 [22], and (Li, Na, K)Cl [23].

As an application of the Klemm method, the discovery of the Chemla effect is worthy of special attention. Chemla tried to enrich lithium isotopes in the mixture system (Li, K)Br and discovered this effect in 1958 [24 – 26]; at the anode side, the ratio Li/K attained to a constant value with time, whereas ^{7}Li (and ^{41}K) continued to be enriched there.

It took almost 20 years for the very amazing phenomenon discovered by Chemla in 1958 [24] to be named the Chemla effect later [4]. As for the definition: A crossing point appears when plotting as a function of two isotherms, for identical temperature T, for the (internal or external) mobilities of two species in a mixture defines, sensu stricto, the existence of a Chemla effect. This definition is more general than stating that a Chemla effect occurs, e.g. in the case of (Li, Na)NO_3, because the larger cation is more mobile than the smaller one under all accessible conditions [5]. In charge symmetrical multivalent cation melts with a common anion such as $(Ca, Ba)_{1/2}Cl$ [27] and $(Y, La)_{1/3}Cl$ [28], the larger cation is more mobile. On the other hand, in the case of (Li, NH_4)NO_3 and (Na, NH_4)NO_3 the definition for the Chemla effect is more difficult since the isotherms cannot cover all the concentration range ($0 \leq x_{NH_4} \leq 1$) owing to the thermal decomposition of NH_4NO_3. In such cases, we propose the following definition, taking (Na, NH_4)NO_3 as an example. In this mixture, the isotherms of the internal mobilities have been measured from ca. $0.7 < x_{NH_4} < 1$ at 160 – 180 °C [29] (as the melting point of NH_4NO_3 is reported to be 169.6 °C [30], it presumably exists as the super-cooled liquid at 160 °C). In this concentration range, NH_4^+ is more mobile than Na^+, but the slopes of the isotherms as a function of the concentration are considerably different. If these two isotherms are extrapolated, these would obviously have a crossing point at $x_{NH_4} \approx 0.5$, where this mixture is not stable. Thus, the definition of the Chemla effect in such a case is proposed to be as follows: when two isotherms are extrapolated through the entire concentration range (including an imaginary range), they would have a crossing point. The Chemla effect rests on the notion of isotherms; therefore, extrapolation with respect e.g. to concentration may be allowed but not with respect to temperature. Even the imaginary region could be easily studied in the future by molecular dynamics (MD) simulation, when suitable potentials have been found. The Chemla effect has so far been found experimentally only for monovalent cation pairs. An anion Chemla effect has been even observed in Li(Cl, NO_3) by the Klemm method [31], although a countercurrent process does not occur for anions.

In order to understand the Chemla effect, the Klemm method has been applied also for measurement of the internal mobility difference of two cations particularly in binary systems with a common anion. For this purpose, the Klemm method is much more adequate than the electromotive force (EMF) method or the (conventional) Hittorf method. In the EMF method, the error becomes large with increasing (or decreasing)

molar ratio of two cations, as pointed out in [32], and in the Hittorf method, the necessary range of unchanged composition between the cathode and anode compartments probably does not exist; the voluminous anode compartment prevents large changes in composition, which may possibly cause a major error [32]. In the zone electromigration method, radioisotopes or enriched stable isotopes have to be employed; a high voltage is usually needed, and the high temperature operations above 500 °C may be difficult.

As the Chemla effect has played a key role for the interpretation of the mechanism of electrolytic transport mechanism in molten salts [33, 34], the Klemm method, useful for accurate measurement of (cation) mobilities in mixtures, has seen its area of application much extended. For example, the dynamic dissociation model has been proposed based on a wealth of data obtained by the Klemm method, again mainly for binary mixtures with a common anion [35–39].

The dynamic dissociation model has been explained in detail in [33–39]. In brief, the internal mobility is assumed to be strongly related to the velocity component of the cation of interest separating it from its reference anion, named the self-exchange velocity (SEV) [40]. In an MD simulation of (Li, Rb)Cl, the SEV of Rb^+ has been calculated to be larger than that of Li^+ in a 1 : 1 mixture, see for example [40]. Thus, the Chemla effect is reproduced in terms of the SEV.

For the separating motion, the role of an anion (named the attractive anion), which is 'tempting' the cation to leave its reference anion, is considered to be important. Thus, as the number density of the common anions around a cation of interest, which is a function of the molar volume, becomes higher, the separating motion occurs more frequently. From many experiments, an empirical equation has been elaborated for the internal mobilities:

$$u = \frac{A}{(V_\mathrm{m} - V_0)} \exp\left(-\frac{E}{RT}\right), \tag{2}$$

where A, E, and V_0 are constants characteristic of the cation of interest, and R is the gas constant. If the anions were uniformly distributed in a melt, the number density of the anions would be proportional to $1/V_\mathrm{m}$. Therefore, V_0 is a factor corresponding to a deviation from the uniform distribution of the common anions around a cation of interest in the local structure. With decreasing cation radius, this deviation is considered to become larger, because the coulombic interaction becomes stronger. Thus, V_0 is assumed to be generally in the following order among the alkali ions:

$$\begin{aligned} V_0(\mathrm{Li}^+) > V_0(\mathrm{Na}^+) > V_0(\mathrm{K}^+) \\ > V_0(\mathrm{Rb}^+) > V_0(\mathrm{Cs}^+). \end{aligned} \tag{3}$$

It should be noted that the data obtained by Chemla's group on the mobilities of (Li, K)Br, in which the Chemla effect was discovered [24], follow (2) very well [37, 38]. The reason is discussed there in detail. Also in molten binary alkali nitrates, the mobilities follow (2) rather well [33].

From (2), it follows:

$$u^{-1} = a(V_\mathrm{m} - V_0), \tag{4}$$

where $a = (1/A)\exp(E/RT)$. At a given temperature, the value of a is constant and generally decreases when going from Li^+ to Cs^+:

$$\begin{aligned} a(\mathrm{Li}^+) > a(\mathrm{Na}^+) > a(\mathrm{K}^+) \\ > a(\mathrm{Rb}^+) > a(\mathrm{Cs}^+). \end{aligned} \tag{5}$$

Equation (4) indicates that the reciprocal value of the internal mobility is a linear function of the molar volume V_m with the slope of a independent of the kind of coexisting cations.

In the dynamic dissociation model, u has in some cases to be modified from (2); this deviation could be accounted for in terms of the free space effect, the tranquilization effect, and the agitation effect. In (Li, Rb)NO_3 and (Li, Cs)NO_3 at considerably high concentrations of $LiNO_3$, the mobilities of Rb^+ and Cs^+ decrease, respectively, with increasing concentration of $LiNO_3$ [4]. This is because the free space becomes too small for the large Rb^+ and Cs^+ ions to move away from its reference NO_3^- anion. Under high pressure, the mobility usually decreases with decreasing molar volume owing to the small free space. The tranquillization effect usually occurs in a charge unsymmetrical binary system such as (Na, $Ca_{1/2}$)NO_3 [35]. Since the interaction between Ca^{2+} and NO_3^- is stronger than that between Na^+ and NO_3^-, Ca^{2+} ions strongly interact with the attractive anion (and the reference anion), and consequently the Ca^{2+} ion acts as a tranquilizer ion on the SEV of the Na^+ ion. In a charge symmetrical system such as (Li, K)$(SO_4)_{1/2}$ [20], the tranquilization effect by Li^+ on u_K occurs, because the coulombic attraction between the small Li^+ ion and the divalent SO_4^{2-} ion is appreciably stronger than that between the K^+ and SO_4^{2-} ion. Also in (Na, K)OH, the

mobility of K^+ is strongly tranquilized by Na^+ [41]; the coulombic attraction of Na – OH is considerably stronger than the one of K – OH, because an OH-ion behaves like a divalent ion in molten salts. The ionic radius of OH^- is rather small; 132 pm(II), 135 pm(IV), and 137 pm(VI) [42]. However, the Chemla effect occurs also in (Li, K)$(SO_4)_{1/2}$ and (Na, K)OH.

An agitation effect occurs, for example, in the above mentioned (Na, $Ca_{1/2}$)NO_3, where the Na^+ plays a role of an agitator on u_{Ca}, which becomes larger than expected from (2) for the divalent charge symmetrical systems. Another type of agitation effect is seen for Tl^+; for example, in (Tl, M)NO_3 (M=alkali ion or Ag^+), Tl^+ renders u_M significantly larger than expected from (2), presumably because of the high polarizability of Tl^+ [43]. It should be stressed that even if (2) does not hold in some cases, the dynamic dissociation model still holds well at least qualitatively, because this model takes into account the perturbation in terms of the free space effect, the tranquilization effect, and the agitation effect.

Although a detailed explanation of the dynamic dissociation model based on MD simulation is given elsewhere [44], it should be mentioned here that Klemm has presented an equation, based on the linear response theory [45], for the calculation of the internal mobilities in a binary additive mixture from MD simulations. Internal mobilities have been calculated in a mixture of (Li, Cs)Cl ($x_{Cs} = 0.9$) on the basis of this equation [46]; the Chemla effect has been reproduced in the SEV. Morgan and Madden have calculated internal mobilities in (Li, K)Cl at 37 points with different concentrations and temperatures using a modified Klemm equation [47], the result of which supports the dynamic dissociation model.

From a standpoint of isotope separation by use of the Klemm method, the heavier isotope is much easier to enrich at the anode than the lighter one at the cathode. High electric density, say $\sim$ few A/cm^2, needed for high enrichment is hard to obtain at the cathode, because complete oxidation of the otherwise electrodeposited metal into the original cation is essentially required there.

In the initial investigations, Klemm enriched ^{6}Li in the cathode compartment, which contained about 1 g of LiCl from 7.3% to 16.1% (the total separation factor: 2.3) in 4.2 d [48] and to 20% in 8 d [49] using the original method, where the run temperature is not particularly mentioned (mp: 614 °C). Enrichment of ^{6}Li to 90% on a large scale has been designed in LiCl by Klemm [50], although it is not mentioned whether this could be put into practice. Benarie has enriched ^{6}Li using a hollow graphite cathode, thus obtained enriched 6 g of LiCl (^{6}Li: 29.2%) [51]. Périé et al. have used a mixture of (Li, K)Br to enrich ^{6}Li from 8% to 50% contained in 2 g of LiBr [26]. He has obtained ^{6}Li (75%) in electromigration for 120 d, and then, in another trial, enriched ^{6}Li from 34% to 95% in 50 d [52].

Its success notwithstanding, the electro-reduction of Li^+ at the cathode, which has to be immediately followed by the oxidation by a flow of gas such as chlorine and bromine, is in the long run still troublesome at high temperature since molten lithium is one of the most corrosive chemical agents known and especially destructive to graphite and carbon [51]. In general, the treatment of molten salts becomes increasingly difficult above $\sim$ 500 °C because of problems with materials, corrosion, energy consumption, and safety.

Thus, an ingenious contrivance is required if one wants to achieve a high enrichment of lighter isotopes with the Klemm method. Such a method has previously been proposed for the enrichment of ^{6}Li at lower temperatures without redox reaction of lithium. Molten $LiNO_3$ is disposed in the separation tube, adjoining at the mouth to a large cathode compartment containing NH_4NO_3 as the catholyte [53 – 55]. In the present study following the previous study [55], a small amount of $NaNO_3$ has been disposed between $LiNO_3$ and NH_4NO_3 to achieve a stable control of the high enrichment, as schematically shown in Figure 3.

In $LiNO_3$, the elementary separation factor is $\varepsilon = 0.0091 - 0.0117$ (286 – 453 °C) and a small positive

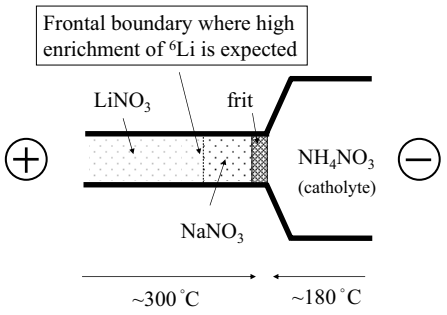

Fig. 3. Schematic representation of the arrangement of $LiNO_3$, $NaNO_3$, and NH_4NO_3 formed naturally near the cathode compartment in the countercurrent experiment.

temperature dependence was also observed in our previous measurement [56], this is 10% – 20% smaller than the one obtained by Lundén and Ekhed [57], who reported

$$\varepsilon = 0.0122 + (2.9 \pm 2.9) \times 10^{-6}(T' - 300)\,, \quad (6)$$

where T' is the temperature in °C. (In their original paper, the value is expressed in the form of the mass effect as $\mu = -0.0845 + (0.00002 \pm 0.00002)(T' - 300)$.) For comparison, in LiCl, $\varepsilon = 0.0194 - 0.0292$ (723 – 895 °C) [58], and in LiBr, $\varepsilon = 0.0202 - 0.0242$ (580 – 615 °C) [59].

Even though the elementary separation factor is considerably smaller in the nitrates than in the halides, many technical difficulties due to high melting points, corrosions, and treatment of the toxic gases can be greatly reduced with the present approach.

2. Experimental

Four long runs of electromigration (Exps. 1 – 4) were performed to enrich ^{6}Li. Another long run of preliminary electromigration experiment (Exp. 5) was performed to learn a possibility of enriching a lighter isotope ^{39}K in a mixture of (Li, K)NO_3 in a similar procedure.

In all runs, molten NH_4NO_3 was used as the catholyte. The melting point of NH_4NO_3 is about 170 °C [30] and it is easily decomposed at higher temperature: 0.12% in 6 h at 170 °C, 15% in 40 min at 240 °C [60]).

2.1. Chemicals

The chemicals $LiNO_3$, $NaNO_3$, KNO_3, and NH_4NO_3 of reagent grade made by Kanto Chemical Co. Ltd. were used; $LiNO_3$, $NaNO_3$, and KNO_3 were vacuum-dried at 120 °C for 24 h before use; NH_4NO_3 was used without further dehydration; because, as one of the thermal decomposition compounds is H_2O [60], the initial dehydration is not likely to be meaningful. Some fundamental properties of these chemicals are given in Table 1.

2.2. Electromigration Cell

The cells shown in Figures 4a and 4b were made of transparent fused silica glass. First the separation tube was built with two cylindrical tubes having different internal diameters (i.d.): 4.3 mm and 12.0 mm; for the smaller part, a thick-walled (ca. 2 mm) tube was used due to mechanical strength requirements. At the mouth of the separation tube to the cathode compartment, a silica frit was installed. Alumina powder of ca. 50 µm was packed as densely as possible as diaphragm inside the separation tube. At the end of the mouth, at the anode side, silica wool was packed and glued to the wall with silica cement (Aron Ceramic C made by Toagosei Chemical, Nagoya, Japan) with attention not to clog the mouth. Although a truncated cone shaped tube may be effective for a smooth countercurrent flow, it could not be employed because of the difficulties to make one in the laboratory. Then, the part of the separation tube was dually covered, as shown in Figure 4a, so that the melt in the separation tube was

Table 1. Some related properties of molten $LiNO_3$, $NaNO_3$, KNO_3, and NH_4NO_3.

		$LiNO_3$	$NaNO_3$	KNO_3	NH_4NO_3
Melting point/°C		254	310	337	170 [a]
Stable isotope (cation)		^{6}Li, ^{7}Li	^{23}Na	^{39}K, ^{40}K, ^{41}K	–
(abundance/%)		7.59, 92.41	100	93.26, 0.012, 6.73	–
Cationic radius/10^2 pm [b]		0.59 (IV)	1.02 (VI)	1.38 (VI)	~ 1.45 (VI)
V_m/cm^3 mol^{-1} [c]	(300 °C)	39.28	(44.50) [d]	53.96	55.74 (170 °C)
	(350 °C)	39.90	45.33	55.01	55.93 (180 °C)
κ/S cm^{-1} [c]	(300 °C)	1.091	(0.944) [d]	0.526	0.368 (170 °C)
	(350 °C)	1.336	1.158	0.661	0.402 (180 °C)
$u/10^{-4}$ cm^2 V^{-1} s^{-1} [c]	(300 °C)	4.44	(4.35) [d]	2.94	2.13 (170 °C)
	(350 °C)	5.52	5.44	3.77	2.33 (180 °C)

[a] 169.6 °C [30].
[b] Except NH_{4+}, the ionic radii are cited from Shannon [42].
[c] The values are calculated from the data book [61]; for NH_4NO_3, the data are taken from [29].
[d] For $NaNO_3$, the values at 300 °C are extrapolated ones, since the melting point is a little higher.

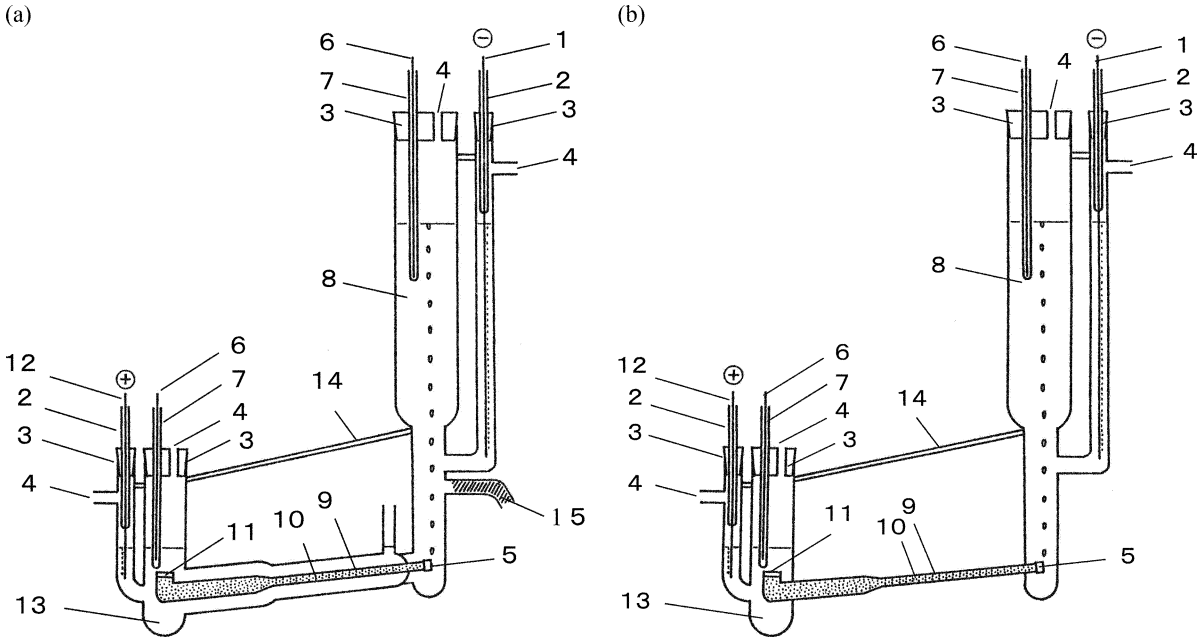

Fig. 4. Electromigration cells. (a) Exps. 1, 3, 4, and 5, see text; only the freezing valve part (15) was installed in Exp. 1. (b) Exp. 2. 1–cathode (Al in Exp. 1 and Pt), 2–Vycor sheath for the electrode, 3–silicone stopper, 4–gas outlet, 5–silica filter, 6–Alumel-Chromel thermocouple, 7–Vycor sheath, 8–molten NH_4NO_3 catholyte, 9–separation tube, 10–alumina powder, 11–silica wool cemented to the wall, 12–Pt anode, 13–molten $LiNO_3$, 14–support bar, 15–freezing valve.

Table 2. Main electromigration conditions.

Experiment No.	1	2	3	4
Separation tube: Length/mm (i.d.: 4.3 + 12 mm)	151 + 118	146 + 107	135 + 119	122 + 119
Amount of salt/g: cathode anode	180	190	150	370
anode	300	160	200	185
Hydraulic head/cm (between cathode and anode)	37 – 40	28 – 33	23 – 28	30 – 35
Voltage/V	80 – 100	90 – 95	100 – 120	100 – 110
Electric current/mA	180 – 280	320	310	500
Current density/A cm^{-2} (i.d. 4.3 + 12.0 mm)	2.3 – 3.6 + 0.30 – 0.46	4.1 + 0.52	2.9 + 0.37	4.3 + 0.54
Temperature/°C (cathode comp.)	180	170	180	180
(anode comp.)	300	300	300	300
Duration/d	41	25	39	34
Transported charge/C	0.74×10^6	0.67×10^6	0.96×10^6	1.18×10^6

heated as uniformly as possible by a melt bath (a part of anolyte), except for Exp. 2, where the separation tube was directly heated by a Nichrome ribbon heater. The cell was made so that the separation tube was slightly tilted (ca. 10°) with respect to the horizontal plane, as shown in Figure 4, for a smoother countercurrent flow and degassing of the thermally decomposed NH_4NO_3 near the end of the tubes. Two heaters of Nichrome tapes were wrapped independently for heating the separation tube (300 °C) and the cathode compartment (170 – 180 °C).

2.3. *Electromigration*

The main experimental conditions of Exps. 1 – 4 are given in Table 2. At first the anode compartment and the separation tube were kept at 300 °C. Dried powder of $LiNO_3$ was put through the anode compartment; the diaphragm part was completely impregnated with the $LiNO_3$ melt in a day. Then, an NH_4NO_3 melt containing about 0.4 g $NaNO_3$ was poured into the cathode compartment (which had been heated beforehand at 170 – 180 °C) to about 5 cm in height. A platinum

wire (diam.: 1 mm) was employed as the anode, while another one (diam.: 1 mm) was used as the cathode in Exps. 2 – 5; aluminium (diam.: 1 mm) was employed in Exp. 1.

The electromigration was started with a current of a few ten mA at first, the current was then gradually increased for about 8 h, while NH_4NO_3 melt was continually added into the cathode compartment up to a predetermined height. During the electromigration, the level of NH_4NO_3 was kept constant with a variation of a few centimetre by feeding there the melt a few times per day. The temperatures of the separation tube and of the catholyte were automatically controlled independently using two Alumel – Chromel thermocouples. Although the melting point of pure $NaNO_3$ is a little higher than the running temperature 300 °C (see Table 1), the zone of $NaNO_3$ did not solidify, presumably because it was mixed to some extent with NH_4^+ and Li^+. For feeding NH_4NO_3 into the cathode compartment, its melt was poured there by taking out the lid ('3' for the catholyte in Fig. 4) shortly without interrupting the electromigration. The transported charge was measured with a coulometer (Hokuto-denko HF-201, Japan).

After electromigration, the melt in the anode compartment was first taken out by tilting the cell, and then the catholyte was removed. The cell was then cooled with iced water; the separation tube was brought out by cutting an outer part of the dual wall (particularly for the cell-type in Fig. 4a).

2.4. Analysis

After the separation tube had been taken out, it was cleaned thoroughly on its outer wall, cut into several fractions of 0.6 – 2.7 cm length, and the content of each fraction was dissolved in pure water for analysis. The quantities of Li^+, Na^+, K^+, and NH_4^+ were measured with an ion chromato-analyser (Yokokawa Denki IC500S) and the isotopic ratios of Li were measured by a surface ionization method with double filaments with a mass spectrometer (Varian MAT 261).

2.5. Some Additional Notes of Each Run

Exp. 1. This was performed with the intention of collecting the samples from the cathode compartment semi-continuously through the frozen tube, as shown in Figure 4a. The exit of the frozen tube was sealed with a Teflon tape during electomigration. About one gram of the catholyte was sampled on alternate days to determine the isotopic ratio of lithium in order to adjust the electric current. Nearly all the catholyte was taken through the frozen tube 5 times during 41 days of electromigration by interrupting the electromigration for a few minutes and heating the frozen part with a gas burner.

As the aluminium wire was used as the cathode, this worked as well as a platinum cathode. The purpose of using an aluminium cathode was to collect continuously enriched lithium as Al-Li alloy. This was not successful, probably because NH_4^+ is preferentially electro-reduced.

Exp. 2. The diaphragm part was directly heated with a Nichrome heater as shown in Figure 4b, whereas, in the other runs, the diaphragm part was indirectly heated in a melt bath, as shown in Figure 4a. Other procedures were similar to the ones in the other runs.

Exp. 3. The diaphragm part was heated by a melt bath, which also played a role of anolyte, as shown in Figure 4a. Other experimental conditions are stated at the beginning of this part.

Exp. 4. When NH_4NO_3 was added up to a height of about 5 cm into the cathode compartment, 0.03 g of $CoCl_2$ was added with the intention of detecting the front region of $LiNO_3$. Sodium nitrate was not intentionally added; however, a small amount of Na^+ seemed to be contained in the diaphragm material as impurity and/or the silica cement, which formed a small zone during the run, as mentioned later in Figure 5c. Other experimental procedures were similar to the ones in Exps. 2 and 3.

Table 3. Main electromigration conditions.

Experiment No.	5
Separation tube: Length/mm (i.d.: 4.3 + 12 mm)	135 + 131
Diaphragm material (Grain size/μm)	Alumina (ca. 50)
Amount of salt/g: cathode	400
anode	180
Hydraulic head/cm (between cathode and anode)	32 – 35
Voltage/V	130 – 160
Electric current/mA	515
Current density/A cm^{-2} (i.d. 4.3 + 12.0 mm)	6.6 + 0.84
Temperature/°C (cathode comp.)	180
(anode comp.)	250
Duration/d	26
Transported charge/C	1.00×10^6

•Expt. No.		1	2	3	4
• The most enriched fraction:	^{6}Li/^{7}Li	0.0926	2.702	10.41	18.60
	^{6}Li/%	8.48	73.0	91.2	94.9
Quantity: N_{Li}/mmol		3.860	0.666	0.181	0.191
• Overall separation factor vs. the feed		1.13	33.9	131	227
• Cathode compartment:	^{6}Li/^{7}Li	0.1060	–	0.1472	0.1021
	^{6}Li /%	9.59	–	12.8	9.27
Quantity: N_{Li}/mmol		86.86	0.643	0.848	0.848
• Anode compartment:	^{6}Li/^{7}Li	0.07962	0.07675	0.07825	0.07782
	(^{7}Li/^{6}Li)	12.56	13.03	12.78	12.85
	^{6}Li/%	7.38	7.13	7.26	7.22
• Original:	^{6}Li/^{7}Li;	0.0818	0.0796	0.0796	0.08183
	(^{7}Li/^{6}Li)	12.22	12.56	12.56	12.22
	^{6}Li/%	7.56	7.37	7.37	7.56
• HETP at the cathode side: h/mm		(8.8)	0.31	0.19	0.20
Length from the boundary/mm [a]		117	94	79	100
Assumed separation coefficient [b]		0.0110	0.0110	0.0110	0.0110

[a] The length of the part (i.d.: 4.3 mm) from the frontal for calculation of the HETP.
[b] The value is taken from [56]. If the value of [57] is taken, $\varepsilon = 0.0122$ at 300 °C.

Table 4. Isotope ratio of lithium and its amount in the most enriched fraction.

Time/d	$Q/10^5$ C	N_{Li}/mmol	N_{Li}/g	^{6}Li/^{7}Li [a]	^{6}Li/%[a]
4	0.77	222	1.54	0.111	9.98
8	1.65	182	1.26	0.086	7.95
18	3.60	150	1.04	0.095	8.69
31	5.83	142	0.98	0.097	8.85
41	7.44	87	0.60	0.106	9.59
Total	7.44	783	5.44	0.099	9.02

[a] Original ^{6}Li/^{7}Li: 0.082 (^{6}Li: 7.54%).

Table 5. Amount of lithium and its isotopic ratio in the totally extracted catholyte in the course of the run (Exp. 1).

Fraction No.	Length/ mm	Internal diam./ mm	N_{Li}/ mmol	N_{Na}/ mmol	N_{NH_4}/ mmol	^{7}Li/^{6}Li[a] (^{6}Li/%)
1	18	4.3	0.006	0.016	2.741	
2	10	4.3	0.002	0.005	1.326	
3	7	4.3	0.001	0.004	1.111	
4	10	4.3	0.017	0.018	1.432	
5	8	4.3	0.666	0.200	0.213	0.3701 (72.99)
6	9	4.3	1.031	0.120	0.019	0.4435 (69.28)
7	10	4.3	0.824	0.038	0.009	0.5609 (64.07)
8	9	4.3	1.359	0.018	0.015	0.7169 (58.24)
9	11	4.3	1.735	0.005	0.018	1.070 (48.31)
10	8	4.3	1.423	0.003	0.022	1.599 (38.48)
11	10	4.3	1.951	0.010	0.002	2.436 (29.10)
12	8	4.3	1.580			3.664 (21.42)
13	11	4.3	2.815			5.487 (15.42)
14	11	4.3	2.758			8.121 (10.96)
15	6	4.3	1.745			10.91 (8.40)
16	12	12.0	11.12			12.74 (7.28)
17	11	12.0	22.38			13.36 (6.96)
18	17	12.0	37.80			13.01 (7.14)
19	13	12.0	28.96			12.94 (7.17)
20	17	12.0	38.95			12.82 (7.24)
21	13	12.0	27.58			12.92 (7.18)
22	24	12.0	52.70			12.94 (7.17)

[a] The original sample: 12.56 (7.37%).

Table 6. Anomalous distribution of lithium isotopes around the region of large temperature gradient (Exp. 2).

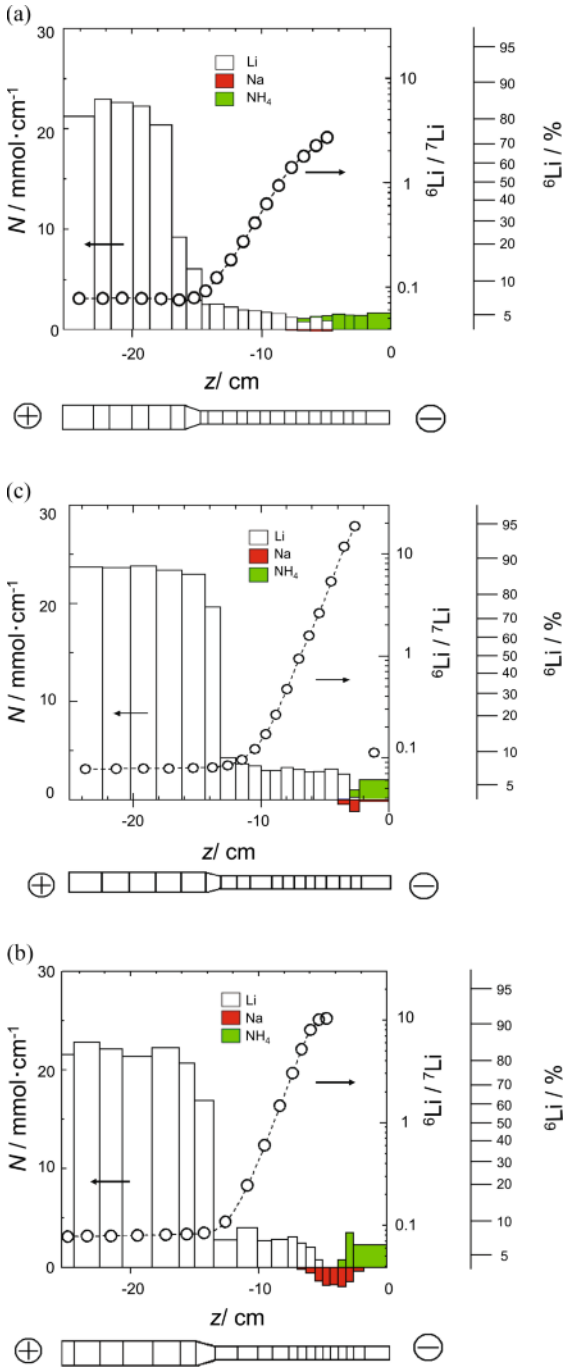

Fig. 5 (colour online). Distributions of the chemical species (left ordinate) and the isotopic ratio of ^{6}Li/ ^{7}Li (right ordinates). (a) Exp. 2, (b) Exp. 3, and (c) Exp. 4. The quantity of $NaNO_3$ is shown in the negative direction for better visibility. The distance z is measured from the frit (included) near the cathode compartment.

Exp. 5. We performed a preliminary run for the purpose of learning a possibility of enriching the lighter isotope ^{39}K using a mixture of (Li, K)NO_3 in a similar cell to the one in Figure 4a for 26 d. The main experimental conditions are given in Table 3. The initial concentration of the mixture (Li, K)NO_3 was chosen to be $x_K = 0.59$, which equals the concentration at the Chemla crossing point of this mixture at the running temperature 250 °C [62] and therefore it was expected that the initial concentration must be kept during the run.

3. Results

The main results of Exps. 1 – 4 are summarized in Table 4.

In Exp. 1, no special attention was paid to keeping the frontal boundary inside the diaphragm part, as the main aim was to collect catholyte containing lithium from the cathode compartment by interrupting the electomigration for a few minutes. The catholyte was sampled through the frozen tube totally five times, including the end of the run. The amount of lithium in this way and its isotopic ratio are given in Table 5. The percentage of ^{6}Li in the most enriched fraction was only of 9.98% (original: 7.54%), in spite of long duration; the electric current flow of lithium seems to have been only a little larger than the countercurrent flow, although the electric current was smaller than in the other runs and the hydraulic head was larger (see Table 2). This result suggests that there was some unequal packing for the diaphragm part of a small diameter (4.3 mm). Among the five present runs, the smaller part was longest in Exp. 1. Even if unequal packing part is present in the larger diameter, it would not disturb the countercurrent flow so much. The long part with a small diameter (4.3 mm) would have caused unsmooth countercurrent flow. This result also shows that the electric current must be well controlled not to overcome the countercurrent flow for high enrichment.

An anomalous distribution of lithium isotopes was found in Exp. 2, as shown in Table 6. This will be explained in section Discussion.

In Exps. 2 – 4, $NaNO_3$ was located around the frontal area of the $LiNO_3$ zone; in Exps. 3 and 4, the zone of $LiNO_3$ was almost completely separated from the one of NH_4NO_3 by $NaNO_3$ (see Figs. 5a – c). This suggests that the enriched ^{6}Li did not escape into the cathode compartment during electromigration. There-

Table 7. Distribution of the cations and the isotopes in the separation tube after a run of (Li, K)NO_3 (Exp. 5).

Fr. No.	L/ mm	i.d./ mm	N_{Li}/ mmol	N_K/ mmol	x^a_{Li}	N_{NH_4}/ mmol	^{6}Li/ ^{7}Li^b (^{6}Li/%)	^{39}K/ ^{41}K (^{39}K /%)
1	14	4.3				1.644		
2	12	4.3	0.511		1	1.477	0.6614 (39.81)	
3	11	4.3	2.366	0.049	0.980	0.510	0.4824 (32.54)	26.46 (96.36)
4	11	4.3	3.077	0.298	0.912	0.064	0.2005 (16.70)	31.94 (96.96)
5	10	4.3	2.641	0.455	0.853		0.1203 (10.74)	29.49 (96.72)
6	15	4.3	3.340	0.741	0.818		0.0789 (7.31)	26.46 (96.36)
7	17	4.3	3.735	0.923	0.803		0.0582 (5.50)	22.08 (95.67)
8	16	4.3	3.507	1.038	0.772		0.0540 (5.12)	18.68 (94.92)
9	14	4.3	2.929	1.027	0.740		0.0547 (5.19)	16.48 (94.28)
10	15	4.3	3.412	1.281	0.727		0.0549 (5.20)	15.52 (93.95)
11	25	12.0	25.52	14.48	0.638		0.0576 (5.45)	14.90 (93.71)
12	20	12.0	17.52	14.75	0.543		0.0629 (5.92)	14.45 (93.53)
13	18	12.0	14.22	15.03	0.486		0.0675 (6.32)	14.23 (93.43)
14	23	12.0	17.46	22.95	0.432		0.0732 (6.82)	14.03 (93.35)
15	25	12.0	13.49	20.73	0.394		0.0767 (6.12)	13.93 (93.30)
16	20	12.0	16.24	26.08	0.384		0.0786 (7.29)	13.86 (93.27)

[a] $x_{Li} = N_{Li}/(N_{Li}+N_K) \approx 0.40$ at the Chemla point at 250 °C [62], and 0.41 (original).
[b] ^{6}Li/ ^{7}Li (original) = 0.0820 (^{6}Li/%: 7.58).

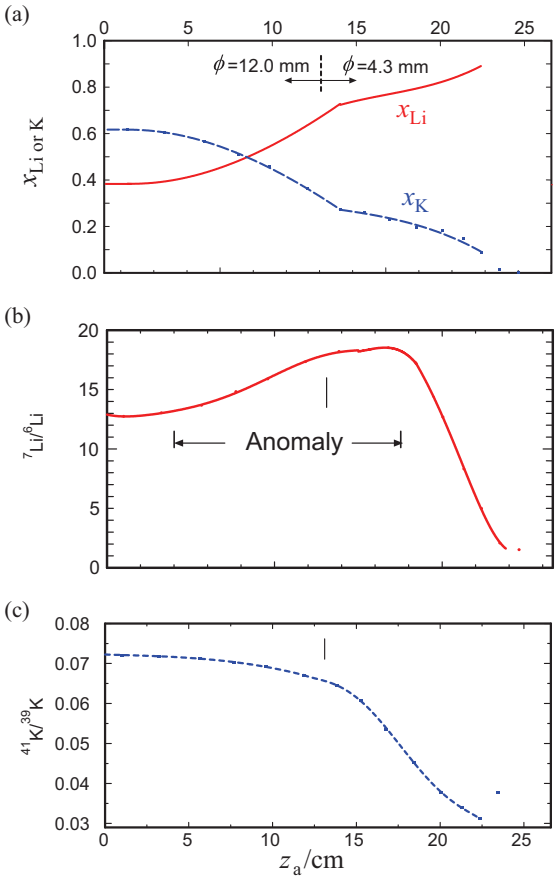

Fig. 6 (colour online). Distributions of the chemical species (a), lithium isotopes (b), and potassium isotopes (c) in Exp. 1. The distance z_a is taken from the end of the separation tube near the anode compartment.

fore, a rather high enrichment of ^{6}Li could be achieved in Exps. 3 and 4.

In Exp. 4, $NaNO_3$ was not added intentionally; however, a small amount of Na^+ was detected in the domain between $LiNO_3$ and NH_4NO_3, as seen from Figure 5c. The origin of this impurity has not been checked. The Na^+-impurity seems to have been concentrated in this domain after a long run, since the mobilities of Li^+, Na^+, and NH_4^+ are of the order shown in Figure 3.

In many trials of similar runs, we have experienced that, when a high electric current is well balanced by the countercurrent flow, a black zone of about 5 mm often appears and remains stationary near the mouth open to the cathode compartment, and ^{6}Li is well enriched. We have assumed that this must be metal oxides such as Fe_2O_3 originating from impurities. Thus, in Exp. 4, a small amount of Co^{2+} was added to the catholyte; $Co(NO_3)_2$ is known to be oxidized directly to Co_2O_3 at 100 – 105 °C [63]. A narrow black zone consequently formed within a few days and stayed there during the run of a month and ^{6}Li was readily enriched. However, this mechanism remains to be studied in more detail.

In Exp. 5, a possibility of enrichment of ^{39}K by the present method using a mixture of (Li, K)NO_3 was examined. Unexpected distribution particularly of the chemical species was observed. The distribution of the chemical species and of their isotopes is shown in Table 7 and Figure 6. This anomalous distribution of the chemical species and the isotopes will be explained in the next section. A small amount of ^{39}K was enriched.

4. Discussion

4.1. Mobility Order of Li^+, Na^+, *and* NH_4^+

It is seen from Figs. 5a–c that the mobility order of Li^+, Na^+, and NH_4^+ ions is, as shown in Figure 3,

$$u_{Li} < u_{Na} < u_{NH_4}\,. \tag{7}$$

It has previously been found that, in (Na, NH_4)NO_3, NH_4^+ is more mobile than Na^+ under all realizable conditions of temperatures and concentrations [29]. Since NH_4NO_3 decomposes thermally rather rapidly above 240 °C [60], as mentioned above, the temperature has to be kept below 180 °C and the concentration of NH_4^+, x_{NH_4}, should be above 0.7, where $u_{Na} < u_{NH_4}$ at high concentrations of NH_4NO_3 [29]. The case is quite similar for (Li, NH_4)NO_3, where $u_{Li} < u_{NH_4}$ [64].

It has previously been studied that in a binary mixture (Li, Na)NO_3, Na^+ is more mobile than Li^+ in all the entire investigated range of temperatures and concentrations [5]: $(u_{Li} - u_{Na})/\langle u\rangle = -0.05 \sim -0.14$. There are ten combinations of binary alkali nitrates (from Li to Cs), among which only in (Li, Na)NO_3 the larger cation is always more mobile than the smaller one [33, 36], i.e., the Chemla crossing point does not exist under accessible conditions at ambient pressure. The case is similar in (Li, Na)Cl [65] and (Li, Na)$(CO_3)_{1/2}$ [66]; but in (Li, Na)Br, a Chemla crossing point appears [26] .

Equations (2) and (4) hold rather well in alkali nitrates. Thus, the condition for a Chemla crossing point to appear in the system (Li, Na)NO_3 is at the smallest molar volume, i.e., in pure $LiNO_3$, (8a) is fulfilled and that at the largest molar volume, i.e., in pure $NaNO_3$, (8b) holds at the same time:

$$a_{Li}(V_{mLi} - V_0(Li^+)) < a_{Na}(V_{mLi} - V_0(Na^+))\,, \tag{8a}$$
$$a_{Li}(V_{mNa} - V_0(Li^+)) > a_{Na}(V_{mNa} - V_0(Na^+))\,, \tag{8b}$$

where a_{Li} and a_{Na} are the values of a of $LiNO_3$ and $NaNO_3$, respectively; V_{mLi} and V_{mNa} are the molar volumes of $LiNO_3$ and $NaNO_3$, respectively, which are given in Table 1.

The values of (8a) and (8b) are calculated from the parameters A, E, and V_0 which have previously been estimated from the ones of various binary mixtures of (Li, M)NO_3 and (Na, M)NO_3 where M are other alkali ions. The values of (8a) and (8b) thus assumed are compared in Table 8. This shows that the necessary condition (8a) for the Chemla effect is not fulfilled, whereas (3) is narrowly fulfilled at 350 °C, as stated below. The main reason is considered to be an irregularly small value of V_0(Li) in comparison with V_0(Na) in the nitrates; $V_0(\mathrm{Li}) = 24.7\,\mathrm{cm^3\,mol^{-1}}$ (nearly independent of temperature) and $V_0(\mathrm{Na}) = 25.3$, 24.2, and $23.2\,\mathrm{cm^3\,mol^{-1}}$ at 327 °C, 350 °C and 400 °C, respectively [5] . This is presumably because the structural position of Li^+ with respect to the planar, triangular shaped NO_3^- ion is different from that of other alkali ions such as Na^+ or Rb^+. From a structural study by X-ray and neutron diffraction as well as MD simulation of $LiNO_3$, it has been found that Li^+ has a high probability of being located in the plane of its NO_3^- neighbour [67]. Another irregular property of $LiNO_3$ in comparison with $NaNO_3$ can also be seen in the mobility data given in Table 1, where u_{Li} in pure $LiNO_3$ is nearly equal to u_{Na} in pure $NaNO_3$. This is in contrast with the chlorides and the bromides, where the mobility of Li^+ melt is much larger than the one of Na^+ melt: for example, at 800 °C, LiCl: $2.05 \cdot 10^{-3}\,\mathrm{cm^2\,V^{-1}\,s^{-1}}$, NaCl: $1.39 \cdot 10^{-3}\,\mathrm{cm^2\,V^{-1}\,s^{-1}}$, and LiBr: $2.25 \cdot 10^{-3}\,\mathrm{cm^2\,V^{-1}\,s^{-1}}$, NaBr: $1.42 \cdot 10^{-3}\,\mathrm{cm^2\,V^{-1}\,s^{-1}}$ [61].

In the present process, even if the countercurrent flow overcame the electric current flow, the catholyte, NH_4NO_3, could not enter deeply in the separation tube, as seen from Figs. 5a–c, owing to its thermal decom-

Table 8. Comparison of the roughly assumed $(1/u_{Li})$ and $(1/u_{Na})$ in pure $LiNO_3$ and $NaNO_3$.

In pure $LiNO_3$		Judgement
$a_{Li}(V_{mLi} - V_0(Li^+))$	$a_{Na}(V_{mLi} - V_0(Na^+))$	
$(1/0.0091)\cdot(39.9–24.7)$	$(1/0.0112)\cdot(39.9–24.2)$	l. h. > r. h.
$[\mathrm{cm^5\,V^{-1}\,s^{-1}}]\cdot[\mathrm{cm^3\,mol^{-1}}] = 1660\,\mathrm{cm^{-2}\,V\,s}$	$[\mathrm{cm^5\,V^{-1}\,s^{-1}}]\cdot[\mathrm{cm^3\,mol^{-1}}] = 1400\,\mathrm{cm^{-2}\,V\,s}$	$u_{Li} < u_{Na}$
In pure $NaNO_3$		Judgement
$a_{Li}(V_{mNa} - V_0(Li^+))$	$a_{Na}(V_{mNa} - V_0(Na^+))$	
$(1/0.0091)\cdot(45.3–24.7)$	$(1/0.0112)\cdot(45.3–24.2)$	l. h. > r. h.
$[\mathrm{cm^5\,V^{-1}\,s^{-1}}]\cdot[\mathrm{cm^3\,mol^{-1}}] = 2260\,\mathrm{cm^{-2}\,V\,s}$	$[\mathrm{cm^5\,V^{-1}\,s^{-1}}]\cdot[\mathrm{cm^3\,mol^{-1}}] = 1880\,\mathrm{cm^{-2}\,V\,s}$	$u_{Li} < u_{Na}$

position at higher temperature there. Therefore, higher hydraulic head may be possible to obtain higher current density, by which, however, the order of (7) will not be disturbed.

4.2. *Anomalous Distribution of the* Li *Isotopes Around the Middle of the Separation Tube: the Lundén Anomaly*

In the Klemm method, the lighter cationic isotope is usually enriched toward the cathode and the heavier one toward the anode.

As seen from Table 6 (Fraction 17) corresponding to Figure 5a for Exp. 2, a significant, anomalous enrichment of ^{7}Li around the boundary region between the larger tube (i.d.: 12.0 mm) and the smaller tube (i.d.: 4.3 mm) is observed, whereas such an anomaly is not explicitly detected either in Exp. 3 or in Exp. 4. The heating method in Exp. 2 is different from the one in Exp. 3 or 4 in that the separation tube was heated directly with a Nichrome tape in the former and more uniformly through a melt bath in the latter. Therefore, in Exp. 2, the temperature must have been appreciably higher in the small tube than in the larger tube owing to the higher Joule heat.

In the previous similar experiments of ^{6}Li enrichment, mentioned above [43], the separation tubes consisted also of two tubes with different diameters, heated directly with a Nichrome tape. In one of the two runs, ^{7}Li was anomalously enriched around the connected part of two tubes (int. diam. 4.5 mm and 10.2 mm); in the most anomalously enriched fraction, $^{7}\mathrm{Li}/^{6}\mathrm{Li} = 14.18$ (initial: 12.40). (In the other run, around the range where anomalous enrichment of ^{7}Li was expected, this enrichment overlapped with the ^{7}Li enrichment at the anode.)

A similar but very small anomaly was discovered in electromigration of pure KNO_3 [68] and pure $LiNO_3$ [57] around the mouth (frit part) of a separation tube opening to a large cathode compartment by Lundén and coworkers; ^{6}Li and ^{39}K were very slightly but significantly enriched. The situation is schematically shown in Figure 7a. In four runs of $LiNO_3$ for 24 h, ^{6}Li has been enriched; the separation factors in Fractions 1 – 3 are given in the legends of Figure 7a.

Later, Klemm and Lundén have interpreted this kind of anomaly [69]. In brief, if the elementary separation factors are different in the neighbouring two loci S and S′ in a pure melt, the isotope enrichment occurs there; here S′ is taken in the cathode direction from S. As shown in Figure 7a, if the temperature T_1 at S is higher than that of T_2 at S′, ε (at S) is greater than ε' (at S′), i.e., $\varepsilon > \varepsilon'$, because the elementary separation factor is positive temperature dependent in such melts as $LiNO_3$ [56, 57] and KNO_3 [68], as mentioned above. In this case, the lighter isotope is enriched there, as shown in Figure 7a; ^{6}Li and ^{39}K were enriched in the case of pure $LiNO_3$ and KNO_3, respectively.

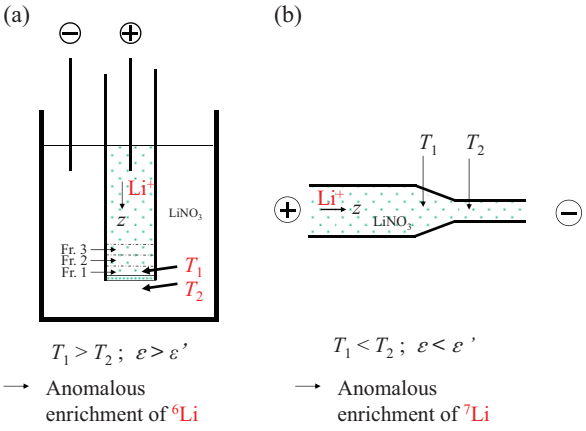

Fig. 7 (colour online). Schematic representation of the occurrence of the first Lundén anomaly. (a) Situation in which the anomaly was discovered [57]; separation factors for four experiments in Fraction 1, Fraction 2, and Fraction 3 were 1.011, 1.012, and 1.010, respectively, (the length of each fraction is not mentioned). (b) Situation in Exp. 2.

On the other hand, in the present case (Exp. 2), the temperature must be lower in the tube of larger diameter; therefore, $\varepsilon_{\mathrm{Li}} < \varepsilon'_{\mathrm{Li}}$, and thus ^{7}Li is expected to enrich there (see also Fig. 7b). In the present experiment, the transported charge is large, and the duration is considerable (25 d), and, therefore, enrichment of ^{7}Li is very clear in a wide range of Fractions 16 – 20, as given in Table 6 (particularly, Fraction 17). In Fraction 16, the enrichment of ^{6}Li toward the cathode may have compensated the anomalous enrichment of ^{7}Li to some extent. Around Fractions 19 and 20, the enriched ^{7}Li at the cathode compartment is likely to overlap the anomalously enriched ^{7}Li.

We will call this kind of anomalous distribution of isotopes the first Lundén anomaly (or the first Lundén effect).

In the present case (Exp. 2), the enrichment of ^{7}Li around the middle part of the separation tube is consid-

erably unfavourable for high enrichment of ^{6}Li, as deduced from Figure 5a and Table 6. Thus, uniform heating of the separation tube is important.

Incidentally, another kind of anomaly had been discovered in a binary mixture (Li, K)$(SO_4)_{1/2}$, also by Lundén's group [20]. In their case, Li^+ was more mobile than K^+, and a significant enrichment of the lighter isotope ^{39}K was observed around the middle of the separation tube, while the distribution of Li isotopes was regular.

This phenomenon will be explained here for the case of (Li, K)NO_3, where K^+ is more mobile; because, in (Li, K)NO_3, in comparison with experimental data [70], these have been analyzed by numerical solutions of differential equations for the flow of the isotopic ions, including the diffusion terms [70]. The results obtained from the calculation have reproduced the experimental results well. The distributions are shown for the chemical species (Fig. 8a), the Li^+ isotopes (Fig. 8b), and K^+ isotopes (Fig. 8c). At $x_{Li}/x_K = 0.427/0.573$ at 380 °C, K^+ is more mobile than Li^+, and consequently dc_{Li}/dz becomes more negative with time, while dc_K/dz becomes more positive. If $dc/dz > 0$ and $dc/dz < 0$, the heavier isotope and the lighter ones are enriched there, respectively [71]. Thus, ^{6}Li is enriched in the region $dc/dz < 0$ except for the anode where $dc/dz \approx +\infty$. Consequently, the enriched ^{6}Li is excessively compensated by the enriched ^{7}Li at the anode, and the 'anomaly' does not explicitly appear sometimes. For K^+ in this case, $dc_K/dz > 0$ everywhere including the anode except for the range where the initial concentration is kept constant: $dc/dz = 0$, and therefore ^{41}K is enriched and the anomaly does not appear.

We will call this kind of anomaly the second Lundén anomaly (the second Lundén effect), which is caused by the concentration gradient in mixtures.

Incidentally, the present method for a high enrichment of ^{6}Li at the frontal boundary may be considered to make use of the second Lundén effect by intuition, because at the sharp boundary, dc_{Li}/dz is close to $-\infty$, where the lighter isotope can be effectively enriched. While in the case of the second Lundén anomaly, the concentration gradient is gradually generated during electromigration, the condition of $dc_{Li}/dz \approx -\infty$ is intentionally set at the early stage of electromigration in the case of the present enrichment of ^{6}Li.

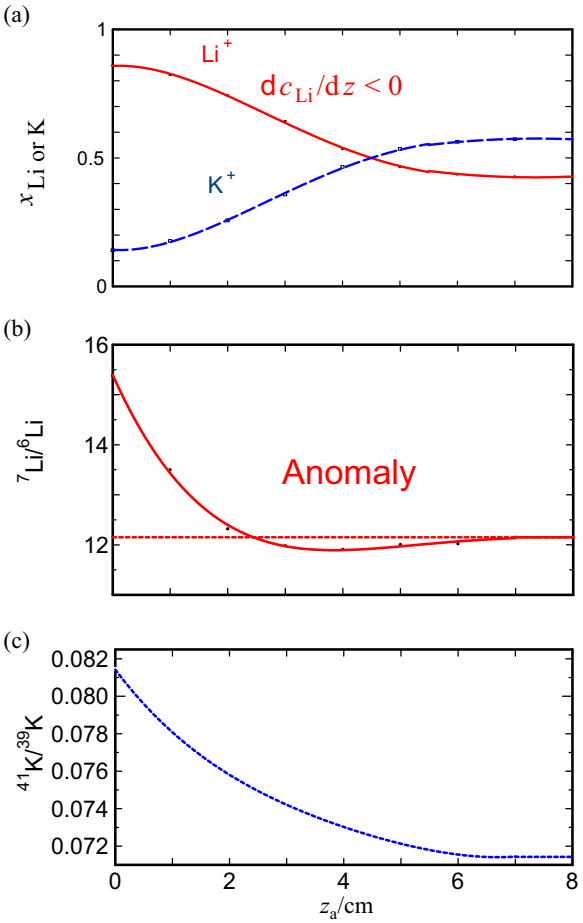

Fig. 8 (colour online). Distributions of the chemical species (a), lithium isotopes (b), and potassium isotopes (c) for the second Lundén anomaly in (Li, K)NO_3. These curves were obtained from the numerical analysis of the experimental results. The distance z is taken from the anode. Initial conditions: $x_{Li}/x_K = 0.427/0.573$, $^7Li/^6Li = 12.15$, $^{41}K/^{39}K = 0.07143$, current density: 2.0 A/cm^2, duration: 15.5 h, Temp. = 380 °C [70].

4.3. Height Equivalent to a Theoretical Plate (HETP)

The HETP h, given in Table 4, has been estimated from

$$h = \frac{\varepsilon \ell}{\ln\{(^6Li/^7Li)_B/(^6Li/^7Li)_A\}}, \tag{9}$$

which is derived from

$$\frac{(^6Li/^7Li)_B}{(^6Li/^7Li)_A} = (1+\varepsilon)^n \tag{10}$$

and

$$h = \ell/n\,. \tag{11}$$

Here ℓ is the distance between locus A and locus B along the z-axis, and n is the number of theoretical plates there. The h values given in Table 4 are calculated only for the smaller part of the separation tube. The values of h are as small as about 0.20 mm in Exps. 3 and 4. On the other hand, the larger part does not explicitly play a role in enrichment; for example, in Exp. 4, the ^{6}Li enriched goes from 7.19% to 7.45% in the larger part of the tube (119 mm), which corresponds to only $n = 3-4$.

This is assumed to be partly due to the first Lundén effect. Although in Exp. 3 and 4, the separation tube was heated by the melt bath, the temperature in the smaller part must have been higher. Although the anomaly is not as explicit here as in the case of Exp. 2, an appreciable enrichment of ^{7}Li must have occurred there. This may be the reason why the larger part of the separation tube did not play an explicit role in the enrichment of ^{6}Li. Thus, the larger tube may be considered to play the role of a reservoir which protects enriched ^{7}Li at the anode compartment from entering directly into the smaller tube. This larger tube would render the countercurrent flow more stable; this is, however, difficult to estimate quantitatively. In Exp. 2, the joint part of the smaller and the larger tubes makes the enrichment of ^{6}Li much less effective, as stated before. In this sense, a truncated-cone shaped or 'pseudo' truncated-cone shaped separation tube may be more effective to obtain a high enrichment of ^{6}Li. Furthermore, a sharp positive temperature gradient in the direction of the migration should be avoided for a high enrichment of ^{6}Li by the present method in the future.

4.4. Possibility of Enriching Lighter Cationic Isotope such as ^{39}K by the Present Method

In Exp. 5, we performed a preliminary run using a mixture of (Li, K)NO_3 ($x_{Li}/x_K = 0.41/0.59$) in a similar cell as in Figure 4a for 26 d.

The apparently strange distribution of the chemical species shown in Figure 6a may be interpreted as follows. As the initial molar fraction ($x_{Li}/x_K = 0.41/0.59$) corresponds to that of the Chemla crossing point at 250 °C [62], the mobilities of Li^+ and K^+ must be practically equal. However, the temperature at the smaller tube must have been higher, as judged from the distribution in Figure 6a. Then u_K must have become larger than u_{Li} in the smaller tube. Further, at the frontal site, where NH_4NO_3 was present, the molar volumes of the ternary mixture are expected to become larger. Equation (2) combined with (3) demonstrates that, when the molar volume becomes larger, the mobility of a smaller cation decreases more sharply than the one of a larger one. Thus, u_K is expected to have become larger than u_{Li} particularly at the frontal area. Although the mobility has not been measured in (K, NH_4)NO_3, the mobility of K^+ may be nearly equal to or greater than the one of NH_4^+ particularly at lower temperature. Therefore, at the early stage of the electromigration, the K^+ ions should preferentially move away into the cathode compartment. This could be supported also from the experimental finding that, in Fractions 1 and 2 in Table 7 (for 26 mm), no K was present. After a large amount of K^+ escaped into the cathode compartment, the mole fraction of Li^+ increased. Since $u_{Li} < u_{NH_4}$, Li^+ did not move away into the cathode compartment. Thus, the following order of these three cations seemed to appear rather soon in the separation tube near the cathode compartment: $u_K < u_{Li} < u_{NH_4}$, as given in Table 7; however, it should be remembered that the difference between u_{Li} and u_K is strongly dependent on concentrations and temperatures, as is indicated by the Chemla effect. Generally, in additive ternary systems, the order of the mobilities is complicated, but they can usually be roughly estimated from (2), where mobility is a function of only the molar volume, i.e., if other parameters such as A, E, and V_0 can be transferred from other systems, and therefore u_{Li} is expected to have become larger than u_K at a relatively early stage of migration.

Figure 6a demonstrates that the distribution of the chemical species discontinuously changes around 14 cm from the anode, which is near the junction point (13.1 cm) of the two different tubes. The temperature increased there, although the separation tube was heated through the melt bath. The temperature dependence of the ratio of u_{Li}/u_K is large; with increasing temperature, the ratio decreases [62], and therefore, the shope of dc_{Li}/dz_a discontinuously decreases, while the one of dc_K/dz_a increases.

The second Lundén anomaly occurred clearly in this experiment for the more mobile Li^+, as seen from Figure 6b; because, as $dc_{Li}/dz_a > 0$, the heavier isotope ^{7}Li was enriched around the middle of the separation tube. As for K^+, $dc_K/dz_a < 0$, the lighter isotope ^{39}K

was enriched over the separation tube. As seen from a comparison of Figures 6a and 6b, the second Lundén anomaly is very unfavourable for high enrichment of ^{6}Li in the vicinity of frontal area of the separation tube.

The HETP is estimated from the isotope ratios of both end fractions; for Li^+, $h = 1.3$ mm ($\varepsilon = 0.0110$ in pure $LiNO_3$ at 300 °C [56]) and for $K^+ h = 0.51$ mm ($\varepsilon = 0.00142$ for ^{39}K – ^{41}K in pure KNO_3 [68]); however, these values are roughly estimated because the elementary separation factors used in the calculation are the ones for the pure melts $LiNO_3$ and KNO_3. Data on the elementary separation factors in mixtures are still limited. Nevertheless, it is evident that, in Exp. 5, the isotope separation efficiency was considerably worse for Li than for K, owing to the second Lundén anomaly.

At the anode side, the chemical composition at the steady state should be the one of the Chemla crossing point. In the present case $x_{Li}/x_K = 0.38/0.62$, while it was $0.41/0.59$ in the feed material, which is nearly equal to the value of the Chemla crossing point at 250 °C. The agreement is satisfactory.

At any rate, ^{39}K could be considerably enriched in this mixture. Since the elementary separation factor is small, one could not highly enrich ^{39}K with only one process. Similarly, ^{85}Rb (72.17%, ^{87}Rb: 27.83) and ^{203}Tl (29.524%, ^{205}Tl: 70.476%) could be enriched to some extent in a binary mixture with $LiNO_3$; these molten nitrates are as stable as $LiNO_3$ and KNO_3, and the isotherms of the mobilities of (Li, M)NO_3 (M = K, Rb, and Tl) are similar in that at high concentration of $LiNO_3$, Li^+ is more mobile than M, and that the Chemla effect occurs [33].

To our knowledge, the distribution of chemical species in binary systems has never been shown at the cathode side in the Klemm method, probably because of the disturbance caused by the cathode reaction. The chemical distribution of the cathode side in additive binary melts or even ternary melts is interesting, particularly when the Chemla effect occurs. Thus, the present method may be employed also for this purpose.

4.5. Lessons from our Experiments

4.5.1. (I) A Proposal for Intermittent Sampling of Highly Enriched ^{6}Li

If one forms a zone of $NaNO_3$ between $LiNO_3$ and NH_4NO_3 for a stable and high enrichment of ^{6}Li, the enriched ^{6}Li does not flow continuously into the catholyte. Consequently, it cannot be sampled during the run. For sampling, when the distribution of the isotopes appears to attain to a steady state, the current is gradually increased to the degree that the countercurrent flow does not compensate the migration flow any more, and enriched ^{6}Li located at a few centimetre from the frontal zone will flow into the catholyte. Then, the electric current is decreased to the former value, and a small amount of $NaNO_3$ is added from the anode compartment or through a hole of a special branch connected to the large diameter part of the separation tube. The Na^+ ion will move rapidly to the frontal part of the separation tube soon.

Another method is to introduce a branch to the separation tube around the boundary region between $LiNO_3$ and $NaNO_3$ for sampling.

4.5.2. (II) Conditions Required for a High Enrichment of ^{6}Li

For a high enrichment, the following conditions are needed, as partly discussed above.

(i) A high current density is essential at a sharp frontal part of the ions of interest, Li^+ in the present case. The formation of a zone of $NaNO_3$ was considered to be useful, since the frontal zone of the $LiNO_3$ was formed inside the separation tube. Otherwise, the frontal zone has to be located near the end of the separation tube open to the catholyte in a large cathode compartment, where the boundary will always be disturbed by the thermal decomposition of NH_4NO_3.

(ii) A high velocity difference in two isotopes Δv ($= E_V \Delta u$) is needed rather than a high mobility difference Δu corresponding to the elementary separation factor; E_V is the applied voltage per length.

(iii) For fulfilling conditions (i) and (ii), a smooth flow of countercurrent is needed. For this purpose, a truncated cone shaped separation tube may be more effective, while in the present runs, two cylindrical tubes were connected. However, it is difficult to estimate the maximum possible flow rate quantitatively through calculation, because it is not only a function of the hydraulic head but also of the packing state of the powders. Thus, it is also difficult to estimate the most effective taper of the tube. These may be more easily solved by trial and error in experiments.

(iv) A sharp temperature positive gradient in the direction of migration should be avoided. Uniform heating of the separation tube is needed.

One problem remains to be solved; if one could find a simple means of detecting the front of $LiNO_3$ in the separation tube on the spot, one could adjust the electric current density to be as high as possible to enrich ^{6}Li more efficiently.

5. Summary and Conclusion

Although the elementary isotope effect is smaller in the nitrate than in the halides, ^{6}Li could be highly enriched at a relatively low temperature (lower than ca. 300 °C) on a laboratory scale without any problem of corrosion; in the most enriched case, ^{6}Li was enriched from 7.6% to 94.9%. A stable zone of $NaNO_3$ between the front of $LiNO_3$ and the main catholyte NH_4NO_3 was formed; for the Na^+/NH_4^+ boundary due to the Chemla effect between $NaNO_3$ and NH_4NO_3, and for the Li^+/Na^+ boundary due to a higher mobility of Na^+ than Li^+ under all conditions in the experiment. Consequently, a sharp front of $LiNO_3$ is created, which is essentially needed for a high enrichment of ^{6}Li. Thus, one problem of the Klemm method, namely that high enrichment of the lighter isotope at the cathode is usually difficult, has been solved for lithium by evading its redox reaction.

An anomalous distribution of isotopes (enrichment of ^{7}Li) in pure $LiNO_3$ in the diaphragm part (not at the anode) has been clearly detected after a long run; this phenomenon is named the Lundén anomaly. This could be accounted for in terms of the temperature difference between two neighbouring two points, as previously suggested by Klemm and Lundén. As this kind of anomaly is unfavourable for a high enrichment of ^{6}Li, a temperature gradient along the separation tube should be avoided.

Acknowledgement

One of the present authors (I. O.) would like to express his sincere gratitude to Professor A. Klemm for invaluable handwritten comments and suggestion on almost all of his papers submitted to Zeitschrift für Naturforschung Teil A. The naming of the self-exchange velocity (SEV) is wholly owed to Professor Klemm, the idea of which has played an important role in the dynamic dissociation model. His gratitude is extended, in particular, to the late Professor A. Lundén (Göteborg) and the late Professor M. Chemla (Paris) for their very warm guidance and support for the study of the present field.

[1] A. Klemm, Z. Naturforsch. **1**, 252 (1946).
[2] A. Klemm, H. Hintenberger, and P. Hoernes, Z. Naturforsch. **2a**, 245 (1947).
[3] M. Chemla, Bull. Soc. Chim. France **14**, 7 (1967).
[4] I. Okada, R. Takagi, and K. Kawamura, Z. Naturforsch. **34a**, 498 (1979).
[5] C.-C. Yang, R. Takagi, and I. Okada, Z. Naturforsch. **35a**, 1186 (1980).
[6] E. P. Honig, Thesis, Amsterdam (1964).
[7] A. K. Brewer, S. L. Madrosky, and J. W. Westhaver, Science **104**, 156 (1946).
[8] A. Klemm, Z. Physik **123**, 10 (1944).
[9] D. H. Whiffen, Pure Appl. Chem. **51**, 12 (1979).
[10] A. Klemm, J. Chim. Phys. **60**, 237 (1963).
[11] A. Klemm, Transport Properties of Molten Salts, in: Molten Salt Chemistry (Ed. M. Blander), Interscience Pub., New York, London, Sydney 1964, p. 535.
[12] A. Klemm and K. Heinzinger, Electromigration in Metals, Salts and Aqueous Solutions, in: Isotope Effects in Chemical Processes, American Chem. Soc., Washington, D.C. 1969, p. 248.
[13] N. Saito, K. Hirano, K. Okuyama, and I. Okada, Z. Naturforsch. **27a**, 288 (1972).
[14] I. Okada, Thesis, University of Tokyo (1966).
[15] H. Matsuura, I. Okada, M. Nomura, M. Okamoto, and Y. Iwadate, J. Electrochem. Soc. **143**, 3830 (1996).
[16] A. Lundén, A. Floberg, and R. Mattson, Z. Naturforsch. **27a**, 1135 (1972).
[17] A. Neubert and A. Klemm, Z. Naturforsch. **16a**, 685 (1961).
[18] C.-A. Sjöblom and R. W. Laity, Z. Naturforsch. **37a**, 706 (1982).
[19] F. Lantelme and M. Chemla, Bull. Soc. Chim. France 2200 (1963).
[20] V. Ljubimov and A. Lundén, Z. Naturforsch. **21a**, 1952 (1966).
[21] J. Habasaki and I. Okada, Z. Naturforsch. **40a**, 906 (1985).
[22] P.-H. Chou, R. Takagi, and I. Okada, Z. Naturforsch. **54a**, 329 (1999).
[23] A. Endoh and I. Okada, Z. Naturforsch. **43a**, 638 (1988).
[24] M. Chemla, French Patent, 1 216 418, Demanded on Nov. 24, 1958.
[25] J. Périé and M. Chemla, C. R. Acad. Sci. **250**, 3986 (1960).

[26] J. Périé, M. Chemla, and M. Gignoux, Bull. Soc. Chim. France **12**, 9 (1961).
[27] H. Matsuura and I. Okada, Z. Naturforsch. **49a**, 690 (1994).
[28] H. Matsuura, I. Okada, Y. Iwadate, and J. Mochinaga, J. Electrochem. Soc. **143**, 334 (1996).
[29] T. Haibara, O. Odawara, and I. Okada, Z. Naturforsch. **44a**, 551 (1989).
[30] E. O. Holmes, Jr., E. O'Connell, and F. Hankland, J. Am. Chem. Soc. **73**, 2885 (1951).
[31] A. Endoh and I. Okada, J. Electrochem. Soc. **137**, 933 (1990).
[32] K. Ichioka, I. Okada, and A. Klemm, Z. Naturforsch. **44a**, 747 (1989).
[33] M. Chemla and I. Okada, Electrochim. Acta **35**, 1761 (1990).
[34] I. Okada, J. Mol. Liq. **83**, 5 (1999).
[35] T. Koura, H. Matsuura, and I. Okada, J. Mol. Liq. **73 – 74**, 195 (1997).
[36] I. Okada, Transport Properties of Molten Salts, in: Modern Aspects of Electrochemistry, No. 34 (Eds. J. O'M. Bockris, B. E. Conway, R. E. White), Kluwer Academic/Plenum, New York 2001, p. 119.
[37] I. Okada and F. Lantelme, J. New. Mat. Electrochem. Syst. **9**, 165 (2006).
[38] I. Okada and F. Lantelme, Z. Naturforsch. **63a**, 1 (2008).
[39] I. Okada, H. Horinouchi, and F. Lantelme, J. Chem. Eng. Data **55**, 1847 (2010).
[40] I. Okada, R. Takagi, and K. Kawamura, Z. Naturforsch. **35a**, 493 (1980).
[41] C.-C. Yang, O. Odawara, and I. Okada, J. Electrochem. Soc. **136**, 120 (1989).
[42] R. D. Shannon, Acta Cryst. A **32**, 751 (1976).
[43] I. Okada and P.-H. Chou, J. Electrochem. Soc. **144**, 1332 (1997).
[44] I. Okada, to appear in: Molten Salts: Fundamental and Applications, Chapter 5: Ionic Transport in Molten Salts (Eds. H. Groult, F. Lantelme), Elsevier.
[45] A. Klemm, Z. Naturforsch. **32a**, 927 (1977).
[46] I. Okada, S. Okazaki, H. Horinouchi, and Y. Miyamoto, Mater. Sci. Forum **73 – 75**, 175 (1991).
[47] B. Morgan and P. A. Madden, J. Chem. Phys. **120**, 1402 (2004).
[48] A. Klemm, Z. Naturforsch. **6a**, 512 (1951).
[49] A. Klemm, Z. Elektrochem. **58**, 609 (1954).
[50] A. Klemm, Angew. Chem. **70**, 21 (1958).
[51] M. M. Benarie, J. Inorg. Nucl. Chem. **18**, 32 (1961).
[52] J. Périé, Thesis, Paris (1965).
[53] I. Okada and N. Saito, J. Nucl. Sci. Technol. **11**, 314 (1974).
[54] I. Okada, Z. Naturforsch. **33a**, 498 (1978).
[55] I. Okada, K. Gundo, M. Nomura, Y. Fujii, and M. Okamoto, Z. Naturforsch. **41a**, 1045 (1986).
[56] A. Endoh and I. Okada, Z. Naturforsch. **42a**, 700 (1987).
[57] A. Lundén and A. Ekhed, Z. Naturforsch. **24a**, 892 (1969).
[58] S. Jordan, R. Lenke, and A. Klemm, Z. Naturforsch. **23a**, 1563 (1968).
[59] A. Lundén, S. Christofferson, and A. Lodding, Z. Naturforsch. **13a**, 1034 (1958).
[60] J. D. Brandner, M. Norman, M. Junk, J. W. Lawrence, and J. Robins, J. Chem. Eng. Data **7**, 227 (1962).
[61] G. J. Janz, J. Phys. Chem. Ref. Data **17**, Suppl. 2, 1 (1988).
[62] A. Lundén, J. Habasaki, and I. Okada, Z. Naturforsch. **42a**, 683 (1987).
[63] C. C. Addison and D. J. Sutton, J. Chem. Soc. Suppl. No. **1**, 5553 (1964).
[64] I. Okada, T. Ayano, and K. Kawamura, Z. Naturforsch. **37a**, 158 (1982).
[65] C.-C. Yang and B.-J. Lee, Z. Naturforsch. **48a**, 1223 (1993).
[66] P.-H. Chou and I. Okada, Molten Salt Forum **5 – 6**, 91 (1998).
[67] T. Yamaguchi, I. Okada, H. Ohtaki, M. Mikami, and K. Kawamura, Mol. Phys. **58**, 349 (1986).
[68] A. Lundén and A. Ekhed, Z. Naturforsch. **23a**, 1779 (1968).
[69] A. Klemm and A. Lundén, Z. Naturforsch. **41a**, 935 (1986).
[70] I. Okada and A. Lundén, Z. Naturforsch. **38a**, 97 (1983).
[71] I. Okada, T. Haibara, O. Odawara, M. Nomura, and M. Okamoto, Z. Naturforsch. **43a**, 1005 (1988).